Development and Field Analysis of a Novel Servo Concrete Bracing System for Deep Foundation Pit Excavation

Wang, Shaochun; Xu, Lei; Zhang, Xuehui; Long, Luyuan ; Zhuang, Xiaoying

DOI
10.3390/ buildings14061674

Publication date
2024

Document Version
Final published version

Published in
Buildings

Citation (APA)
Wang, S., Xu, L., Zhang, X., Long, L., & Zhuang, X. (2024). Development and Field Analysis of a Novel Servo Concrete Bracing System for Deep Foundation Pit Excavation. *Buildings*, *14*(6), Article 1674. https://doi.org/10.3390/ buildings14061674

buildings

MDPI

Article

Development and Field Analysis of a Novel Servo Concrete Bracing System for Deep Foundation Pit Excavation

Shaochun Wang [1], Lei Xu [1], Xuehui Zhang [2,*], Luyuan Long [2] and Xiaoying Zhuang [3]

[1] Shanghai Construction No. 1 (Group) Co., Ltd., Shanghai 200120, China; wsc@sclgc.com.cn (S.W.); xl@sclgc.com.cn (L.X.)
[2] Geo-Engineering Section, Department of Geoscience and Engineering, Delft University of Technology, 2628CN Delft, The Netherlands; l.long-2@student.tudelft.nl
[3] Department of Geotechnical Engineering, College of Civil Engineering, Tongji University, Shanghai 200092, China; xiaoyingzhuang@tongji.edu.cn
* Correspondence: x.zhang-10@tudelft.nl

Abstract: This study demonstrates the design and field implementation of an innovative servo concrete bracing system in foundation pit excavation. The bracing system comprises concrete struts, revised purlins, and hydraulic jacks, and its field performance is evaluated in a deep foundation pit project in Shanghai, China. The field measurements demonstrate that the servo bracing system effectively reduces the maximum lateral displacement of the retaining wall by up to 31%. Moreover, the servo jacks modify the wall's flexural behavior by introducing local inflection points at certain depths and driving the displacement peak upward. Furthermore, the system's performance varies with strut configuration, and servo forces influence not only the corresponding acting strut but also the adjacent struts' behavior, implying that the monitoring scope should be expanded when applying the servo bracing system in actual engineering. This study provides a meaningful technical reference for future servo concrete bracing system applications in foundation pit engineering.

Keywords: braced excavation; diaphragm wall displacement; foundation pit; proactive displacement control; underground construction; servo concrete strut

Citation: Wang, S.; Xu, L.; Zhang, X.; Long, L.; Zhuang, X. Development and Field Analysis of a Novel Servo Concrete Bracing System for Deep Foundation Pit Excavation. *Buildings* **2024**, *14*, 1674. https://doi.org/10.3390/buildings14061674

Academic Editor: Duc-Kien Thai

Received: 10 March 2024
Revised: 22 May 2024
Accepted: 1 June 2024
Published: 5 June 2024

1. Introduction

Ground deformation control has always been a critical issue in deep foundation pit excavation. Generally, soil excavation triggers significant unloading effects on the greenfield and is often associated with observed ground disturbance issues [1,2]. If not controlled properly, the resultant deformation tends to impact nearby ground and underground infrastructures [3–8]. For instance, the foundation pit excavation may cause the settlement and tilting of the nearby existing building [9]. Moreover, the excavation process triggers movements of the surrounding soil layers, which may further damage the close pipe gallery and deform the proximity tunnel significantly, which deteriorates its structure integrity [8,10,11]. For controlling adverse ground deformation, it is crucial to design and implement a safe and reliable bracing system during foundation pit excavation.

Generally, the external retaining structure plus internal supports is the dominant bracing system for deep foundation pit excavation, especially in soft ground. This type of bracing system mainly consists of earth-retaining structures (e.g., secant piles, diaphragm walls) and internal support components (e.g., steel and concrete struts) [12]. Reinforcement concrete or steel struts are the mainstream internal support types, and they are typically placed horizontally, functioning as axially bearing rods to resist the lateral deformation of the earth-retaining structures. Mostly, the normal concrete or steel struts are considered as passive bearing parts because their axial bearing capacity is only passively activated by the occurred lateral displacement of the earth-retaining structures [12–14].

This implies that the strut axial forces cannot be proactively adjusted to the changing excavation conditions, and therefore exhibit limitations in ground deformation control.

To address the defects of normal passive struts, servo steel struts have been developed and applied in foundation pit engineering. Generally, servo struts are set up by combining the normal steel struts with hydraulic jacks placed on either or both ends of the strut, and thus, the axial forces can be adjusted conveniently by setting the hydraulic pressures. The servo steel struts have been applied in many deep excavation projects and demonstrated their effectiveness in mitigating ground deformation [15–18]. However, previous studies mainly focus on developing servo steel struts, while there have been very rare studies of servo concrete struts. Considering that concrete struts are widely used especially in mega foundation pit excavations, it is technically necessary to explore applying servo technology to concrete struts.

This study demonstrates the design and implementation of the first servo concrete bracing system worldwide and evaluates its technical performance through field monitoring in an actual foundation pit project. In the rest of this paper, Section 2 presents background project information incorporating the site's geological conditions and normal bracing structure designs. Section 3 details the servo concrete bracing system, including configurations of the servo system, integration of jack-concrete struts, and the control process. Section 4 presents deep insights into the field monitoring results, and further assesses the application performance of the servo bracing system, and finally, Section 5 concludes the study.

2. Engineering Background

2.1. Overall Project Information

The foundation pit in this study is excavated to construct the basement of a (residential and business district) property development project in Shanghai, China. This foundation pit has a total plane area of about 58,000 m^2 and a maximum excavation depth of about 22.1 m below the ground surface (BGS). In the excavation process, the foundation pit is divided into 18 subzones using diaphragm walls for sequential construction planning. In this study, the field monitoring investigation is focused on the area consisting of 8 subzones, namely Z1 to Z4 and Z5a to Z5d, as illustrated in Figure 1. The excavation depths of each subzone are as follows: Z1 area has a depth of 22.1 m BGS, Z2 to Z4 19.9 m BGS, and Z5a to Z5d about 12.4 m BGS.

Since areas of Z5a to Z5b have much smaller excavation depths than areas of Z1 to Z3, they are divided using partition diaphragm walls and designed to have independent bracing structures, as shown in Figure 2. Notably, this foundation pit is located within the displacement-sensitive urban area in Shanghai, with many important existing surrounding facilities that need high attention. Beneath the West Yangsi Road located on the north side of the pit, two in-service metro transit tunnels exist, which are segmented bored tunnels with an outer diameter of 6.2 m, and the nearest upline tunnel is about 9.2 m distant from the external pit boundary (see Figures 1 and 2). On the east side of the pit is Jiyang Road, where many municipal pipelines (energy, telecommunication, electricity) are extending beneath the road. Overall, the pit excavation encounters significant technical challenges revolving around the ground deformation control and disturbance mitigations to surrounding facilities.

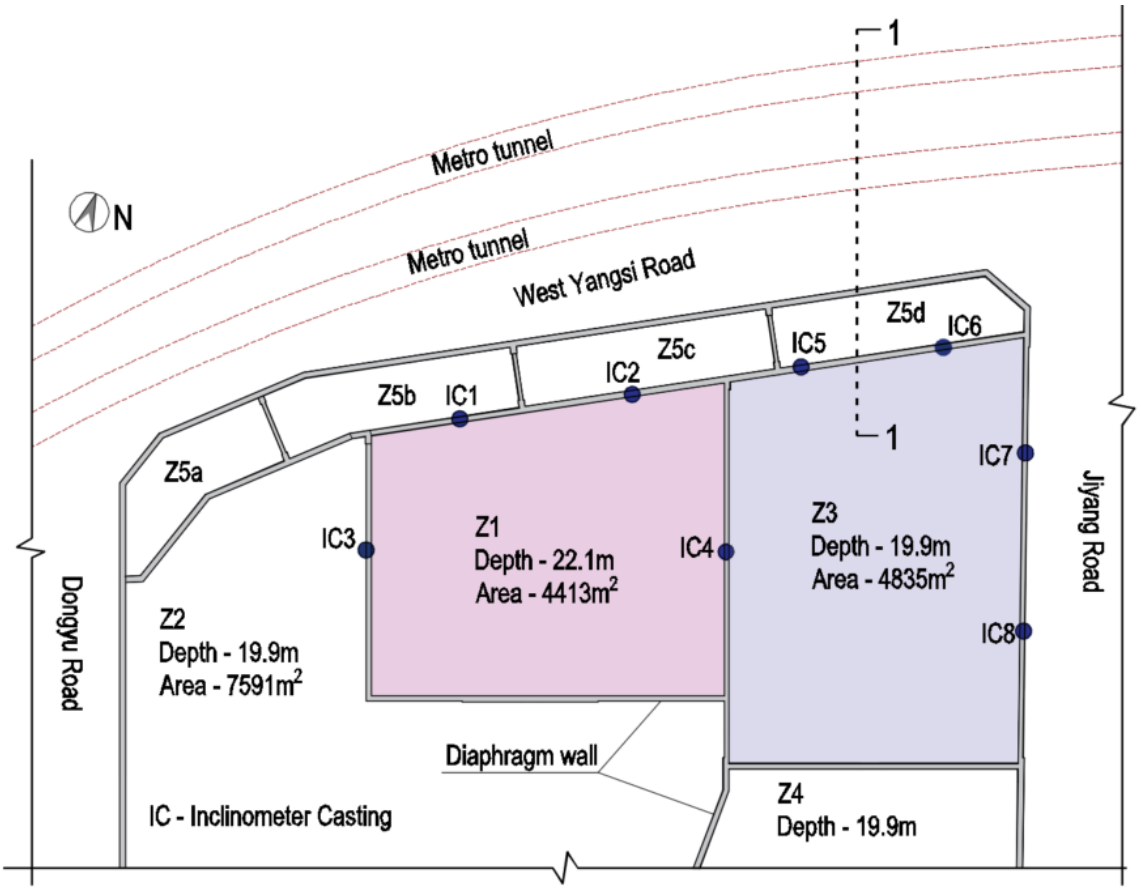

Figure 1. Plane view of the foundation pit project.

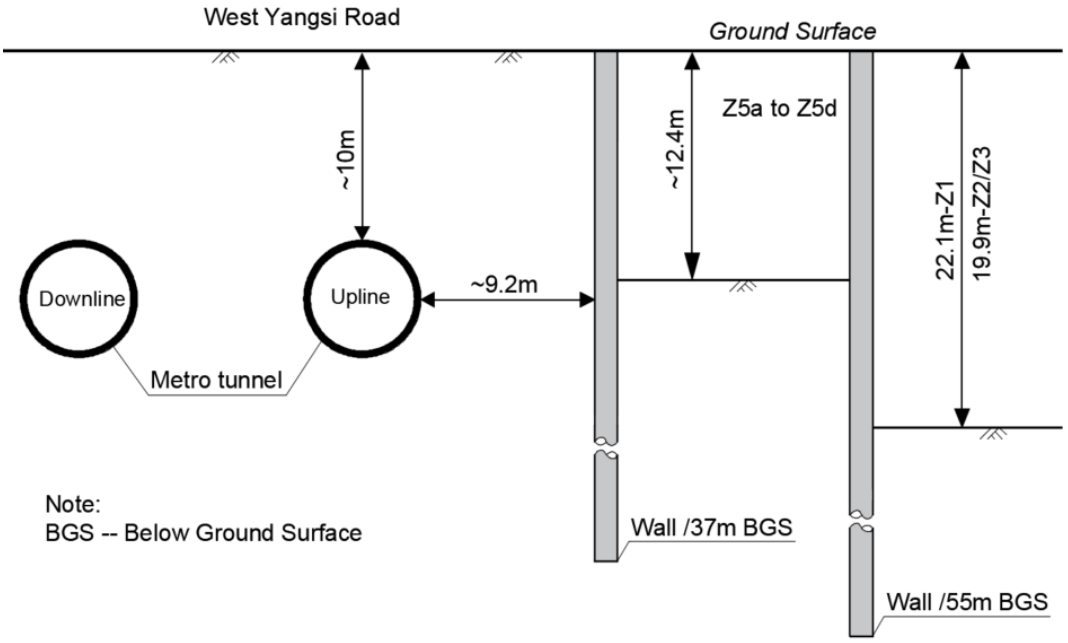

Figure 2. Section view of the foundation pit (1-1 cross-section).

2.2. Site Geological Conditions

The site is located in the southeast front of the estuary of the Yangtze River Delta, and the geomorphic unit belongs to the coastal plain. According to the site geotechnical condition investigation, the stratum within the influence depth of the foundation belongs to

the Quaternary Holocene to Middle Pleistocene coastal plain sedimentary soil layer of the Yangtze River Delta, which is mainly composed of clayey soil, silty soil, and sandy soil. According to the soil genetic type, spatial distribution, and geotechnical properties, the ground strata within the construction site are divided into ten layers from top to bottom.

There is no surface water distribution at the site, and the phreatic water in the shallow soil layer directly influences the pit construction of this project. The stable water level in the borehole measured is about 0.6~1.6 m below the ground surface. Moreover, according to the field investigation, the micro-artesian water level at the site is about 7.1 m below the ground surface. The soil strata and their corresponding geotechnical parameters are detailed from top to bottom in Table 1. Note that in the table, the static earth pressure coefficient refers to the ratio of horizontal to vertical effective stress of the soil, measured through laboratory consolidation tests. The subgrade reaction stiffness is defined as the force causing a unit settlement of ground soil, typically measured using field plate loading tests. $E_{s(0.1-0.2)}$ means the compressive modulus of soil at a stress level of 0.1~0.2 MPa. The soil mechanical properties are determined according to the Chinese geotechnical surveying code [19,20].

Table 1. Table of geotechnical parameters.

Soil Type	Strength Parameters		Density γ (kN/m³)	Saturation *Sr* (%)	Void Ratio *e*	Static Earth Pressure Coefficient K_0	Permeability Coefficient K (cm/s)	Subgrade Reaction Stiffness (kN/m⁴)	Compression Modulus $E_{s(0.1-0.2)}$ (MPa)
	C (KPa)	φ (°)							
Silty clay	21	19	18.6	96	0.891	0.50	3.5×10^{-6}	3000	4.73
Muddy silty clay	11	19	17.3	99	1.243	0.56	8.6×10^{-6}	1500	3.02
Clayey silt	7	31	18.7	96	0.850	0.40	2.2×10^{-4}	3000	7.94
Muddy clay	10	13	16.4	96	1.499	0.60	4.2×10^{-6}	1500	1.96
Clay	14	12	17.2	96	1.238	0.55	5.7×10^{-6}	2000	2.80
Silty clay	6	32.5	18.6	95	0.858	0.41	3.0×10^{-4}	4000	8.38
Silty sand	4	34.0	18.7	96	0.830	0.41	3.0×10^{-4}	4000	8.87
Silty clay interbedded with silty soil	15	19.5	18.3	96	0.955	0.56	1.3×10^{-5}	2500	4.43
Silty sand	4	35	18.8	95	0.807	0.41	3.0×10^{-4}	4500	8.25
Silty sand	2	35.5	18.9	95	0.771	0.39	4.0×10^{-4}	7000	9.68
Muddy silty clay interbedded with sandy silt	17	21	18.4	96	0.915	0.54	3.6×10^{-5}	3000	5.91

2.3. Bracing Structure Design of the Foundation Pit

The foundation pit is divided into 18 zones for staged excavation, using diaphragm walls of 0.8 m/1.0 m/1.2 m thickness as partitions and ground-retaining structures. Following the completion of wall construction, jet-mixing grouting is conducted to reinforce the soil inside the pit before excavation. The excavation follows a specified sequence from Zones Z1 to Z4, with Z1 being the first to excavate until the bottom slab level, followed by internal structure construction and backfilling to surface level. Afterward, it is succeeded by the sequential excavation and backfilling of Zones Z4, Z2, Z3, and lastly, the shallow pits Z5a to Z5d. This study focuses on monitoring the excavation of Z1 and Z3, where depths reach 22.1 m and 19.9 m, respectively. Before excavation, soil reinforcement via triaxial jet-mixing extends to a depth of about 27 m BGS in zones Z5b to Z5d, and closer to the diaphragm wall within a 10m distance inside Z1 and Z3.

Within Z1 and Z3, five reinforced concrete (RC) struts are constructed as internal support, descending from the top with varying cross-sectional dimensions illustrated in Figure 3. The first RC strut has a cross-section that is 0.8 m wide and 0.9 m high, while the

other four RC struts are 1.0 m wide and 1.0 m high (see Table 2). A concrete purlin along the pit's perimeter connects to the diaphragm wall, minimizing the effects of concentrated forces from the struts. Dimension differences in strut parameters between Z1 and Z3 are minor. Notably, in Z1 only normal concrete struts are used, whereas in Z3 an innovative servo hydraulic jack system is explored to investigate its performance, which is detailed further in Section 3.

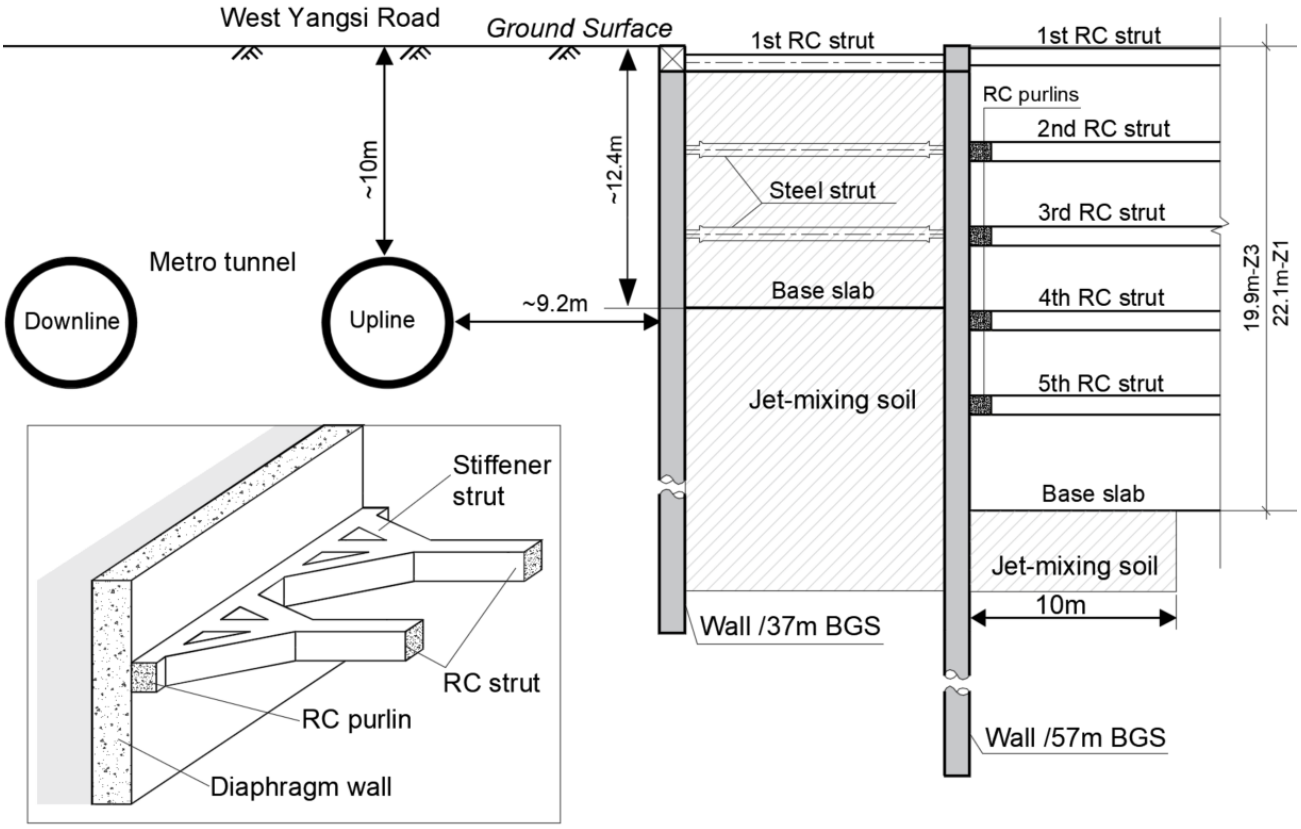

Figure 3. Bracing structure design of the foundation pits: (in lower left corner is strut–purlin–wall connection).

Table 2. Concrete struts information.

Strut	Cross-Section (Width × Height, mm)		Depth (m) /BGS	
	Z1	Z3	Z1	Z3
1st RC strut	800 × 800	800 × 800	0.6	0.6
2nd RC strut	1000 × 900	1000 × 1000	5.1	4.6
3rd RC strut	1000 × 1000	1100 × 1100	9.1	8.4
4th RC strut	1000 × 1000	1000 × 1000	13.1	12.2
5th RC strut	1100 × 1000	1000 × 1000	17.1	16.1

3. Servo Concrete Bracing System Design and Field Implementation

3.1. Configuration of Servo Concrete Bracing System

For a typical bracing structure with concrete struts, a purlin is cast along the perimeter of the retaining wall to evenly distribute the load between the diaphragm wall and the struts, as shown in Figure 3. When combining the servo hydraulic jacks with the concrete struts, several technical issues must be considered, involving, for example, the ease of installation and the need to prevent cracking of concrete when under a concentrated jacking force. To address these issues, a reinforced concrete purlin with an expanded cross-section is meticulously designed and cast on site. Additionally, a series of grooves are constructed

within the purlin on the side near the diaphragm wall (shown in Figure 4). These uniform-spaced grooves are intended to accurately accommodate the hydraulic jack cluster, ensuring that the servo forces are evenly distributed across the entire purlin. The primary components including reinforced purlins, concrete struts, servo hydraulic jacks, and a hydraulic pumping station, have been carefully designed to meet the performance requirements of the overall servo bracing system. The final field implementation of this system configuration is schematically depicted in Figure 4.

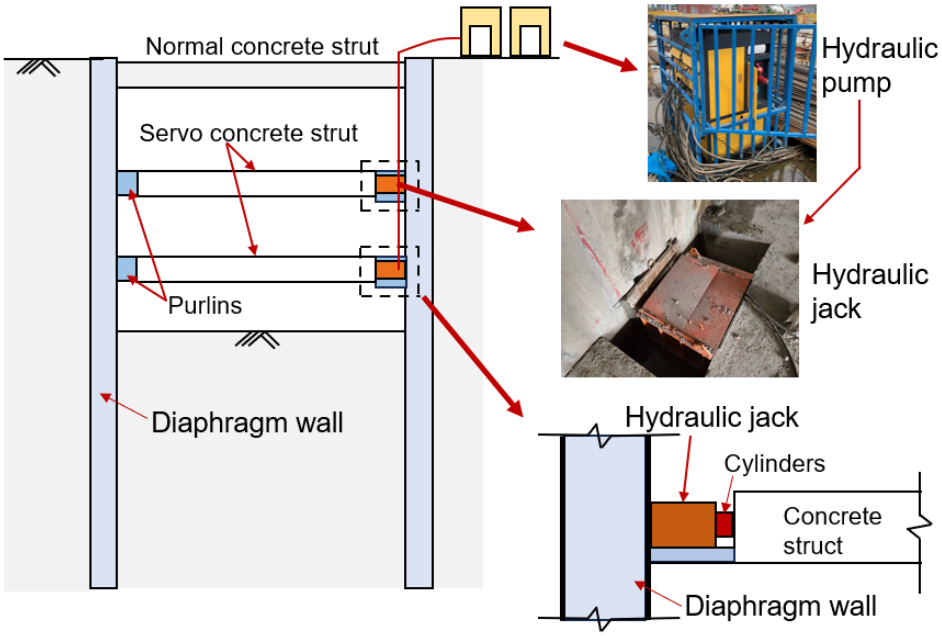

Figure 4. Servo concrete strut design and field implementation.

3.2. Field Implementation

In this project, the designed servo struct is applied in foundation pit Z3, where a total of 48 hydraulic jacks are configured to the third, fourth, and fifth struts (16 jacks each) on the north side facing the West Yangsi Road (see Figure 5b), while 24 hydraulic jacks are configured to the fourth strut on the east side near Jiyan Road (see Figure 5c).

The actual field implementation of the servo bracing system is demonstrated in Figure 6. Firstly, a reinforced concrete purlin is cast on site with discrete grooves (see Figure 6a), and the hydraulic jacks are placed afterward when the concrete hardens (see Figure 6b). Once the servo hydraulic jacks are activated, additional reaction forces are imposed on the diaphragm wall, while the force magnitudes can be adjusted manually according to the control requirements of lateral displacement. The hydraulic forces control operation should consider two aspects: first, the force level should not be too high to incur a significant separation between the diaphragm wall and the purlins; second, the total axial forces (including the additional jack forces) of the concrete struts should not exceed its maximum bearing capacity. In practice, dense field monitoring is conducted with a half-day interval to provide instant feedback on hydraulic force control.

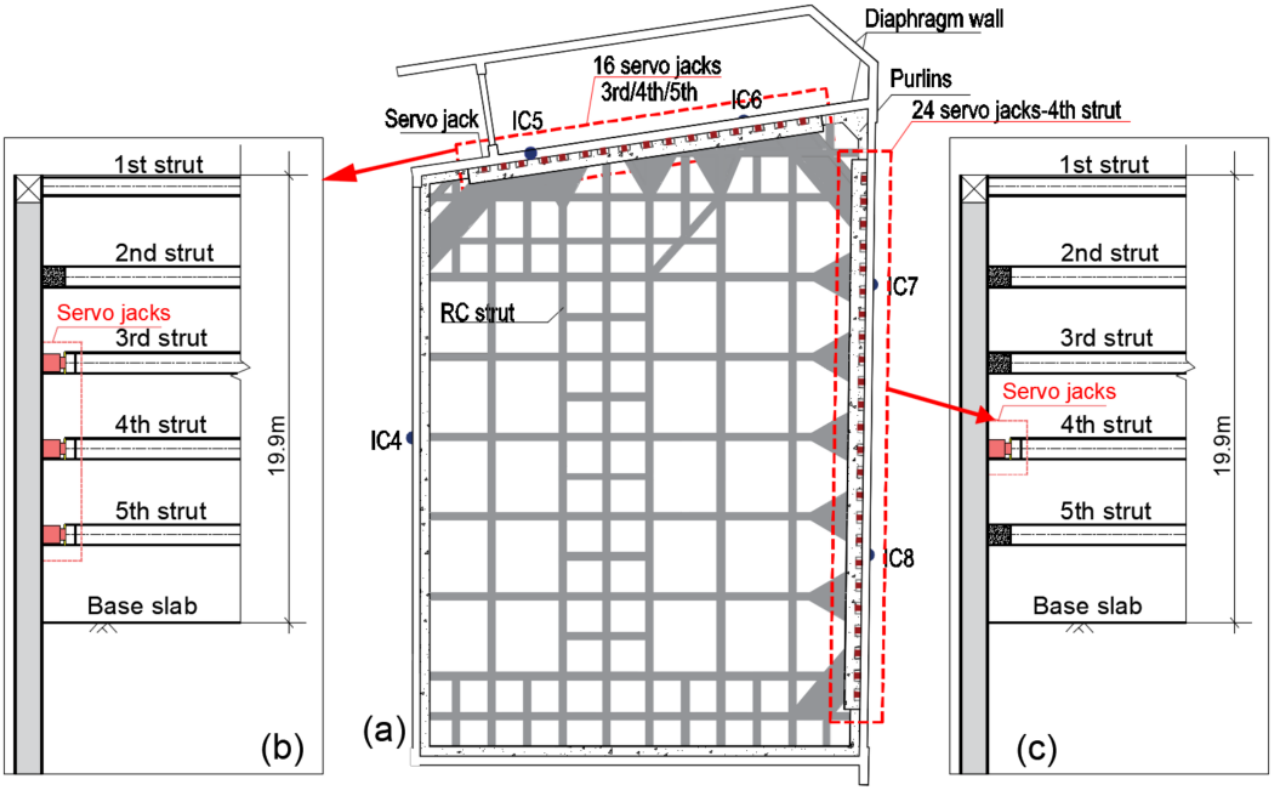

Figure 5. Bracing structure design of the Z3 with servo concrete struts: (**a**) top view; (**b**) cross-section of north side; (**c**) cross-section of east side.

Figure 6. Bracing structure design of the Z3 with servo concrete struts: (**a**) reinforcement cage of purlin; (**b**) field construction of servo RC struts; and (**c**) servo-hydraulic jack.

4. Field Monitoring Result and Discussion

In the foundation pits Z1 and Z3, intensive monitoring is conducted to feedback on the excavation process and ensure safety, compassing the diaphragm wall lateral displacement measured using inclinometer castings (ICs), strut internal forces, and jack forces et al. The excavation of pit Z1 started in October 2020 and was completed to the base slab level by the end of November 2020, followed by the subsequent basement construction; the excavation of pit Z3 started in May 2023, and was finished to the base slab level by the end of July 2023. In this study, the wall lateral displacements of Z1 and Z3 are analyzed and compared to investigate the performance of the servo bracing system.

4.1. Wall Lateral Displacement Monitoring Results

4.1.1. Wall Displacement Results

The wall lateral displacement is measured by inclinometer castings (ICs, with a measure precision of 0.01 mm) initially attached to the reinforcement cage and buried into the diaphragm walls. Four measurement points of foundation pit Z1, namely IC1 to IC4, are selected to investigate the wall deformation throughout the excavation process. The recorded displacement along with depth in Z1 is shown in Figure 7. Note that, in the displacement curves, the dotted arrow lines indicate the elevations of the struts and a depth of 19.9 m (the excavation depth of pit Z3), and each plot corresponds to the lateral displacement of the wall at the time stage when the strut is concreted, while the latest plot (the plot exhibiting the maximum displacement) is measured at the depth of 19.9 m.

Observing the deformation data in Z1, it can be found that the overall wall displacements increase significantly along with the excavation depth. For example, at IC1 the maximum displacement is of about 22 mm when excavating to the second strut level (5.1 m BGS) and increases to about 54 mm at the excavation depth of 19.9 m BGS; at IC3, the maximum displacements are of about 44 mm and 166 mm to the depth of 5.1 m and 19.9 m BGS, respectively. In addition, at each plot the depth of peak displacement is mostly below the excavation depth; for instance, at IC1, the peak value of 22 mm occurring at 13.5 m BGS corresponds to the excavation depth of about 5.1 m BGS, and the peak value of 54 mm occurring at 21.5 m BGS to the excavation depth of about 19.9 m BGS.

Furthermore, the wall displacements demonstrate a significant spatial variation. As can be shown in Figure 7, at the same excavation depth, the wall displacements of points IC1 and IC2, which are adjacent to West Yangsi Road, are much smaller than those of points IC3 and IC4 far away from West Yangsi Road. The maximum displacements (at a depth of 19.9 m BGS) at IC1 and IC2 reach about 54 mm and 42 mm, respectively, while at IC3 and IC4 they are recorded as high as 165 mm and 132 mm. Considering the bracing structure layout, the main reason for this difference may be that IC1 and IC2 are close to the outermost diaphragm wall, which surrounds the shallow foundation pits Z5a to Z5d, and these external walls (with a thickness of 1.2 m) serve as additional ground-retaining structures when pit Z1 is excavated, which reduces the ground deformation significantly. While at IC3 and IC4, there are no external walls offering such additional ground support, and hence a significantly larger deformation.

For the foundation pit Z3 illustrated in Figures 1 and 5, it should be mentioned that the servo jack system is implemented on the third to fifth concrete struts on the north side (facing the metro tunnel lines), with two measurement points IC5 and IC6 on the wall. On the east side adjacent to the energy pipe beneath Jiyang Road, the servo jacks are installed only on the fourth strut, and two measurement points IC7 and IC8 are sampled, with wall lateral displacement results demonstrated in Figure 8.

The displacement results in Figure 8 demonstrate similarities with those in Figure 7, in that overall wall displacements increase significantly with the excavation depth. For example, at IC5 the maximum displacement is of about 9.5 mm when excavating to the second strut level (4.6 m BGS), and further increases to about 42 mm at the excavation depth of 19.9 m BGS; at IC7, the maximum displacements are of about 10 mm and 67 mm

to the excavation depths of 4.6 m and 19.9 m BGS, respectively. Moreover, the displacement results still show spatial variation, since at IC7 and IC8 the wall exhibits a more significant deformation than that at IC5 and IC6. However, highlighted differences exist within the displacement results demonstrated in Figures 7 and 8, which reveal the effects of the servo hydraulic jack system.

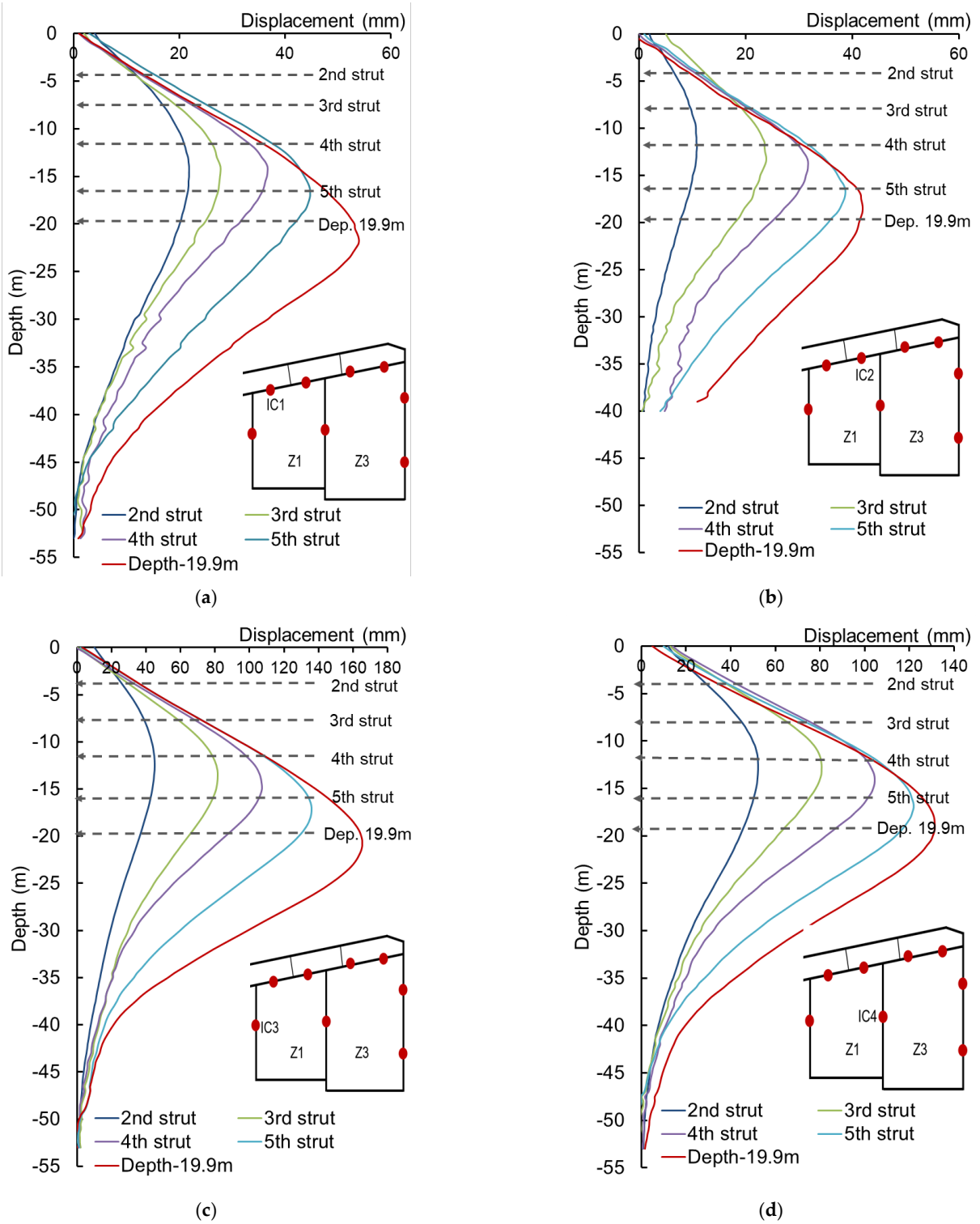

Figure 7. Horizontal displacement results of the diaphragm wall in foundation pit Z1: (**a**) Point IC1; (**b**) Point IC2; (**c**) Point IC3; (**d**) Point IC4.

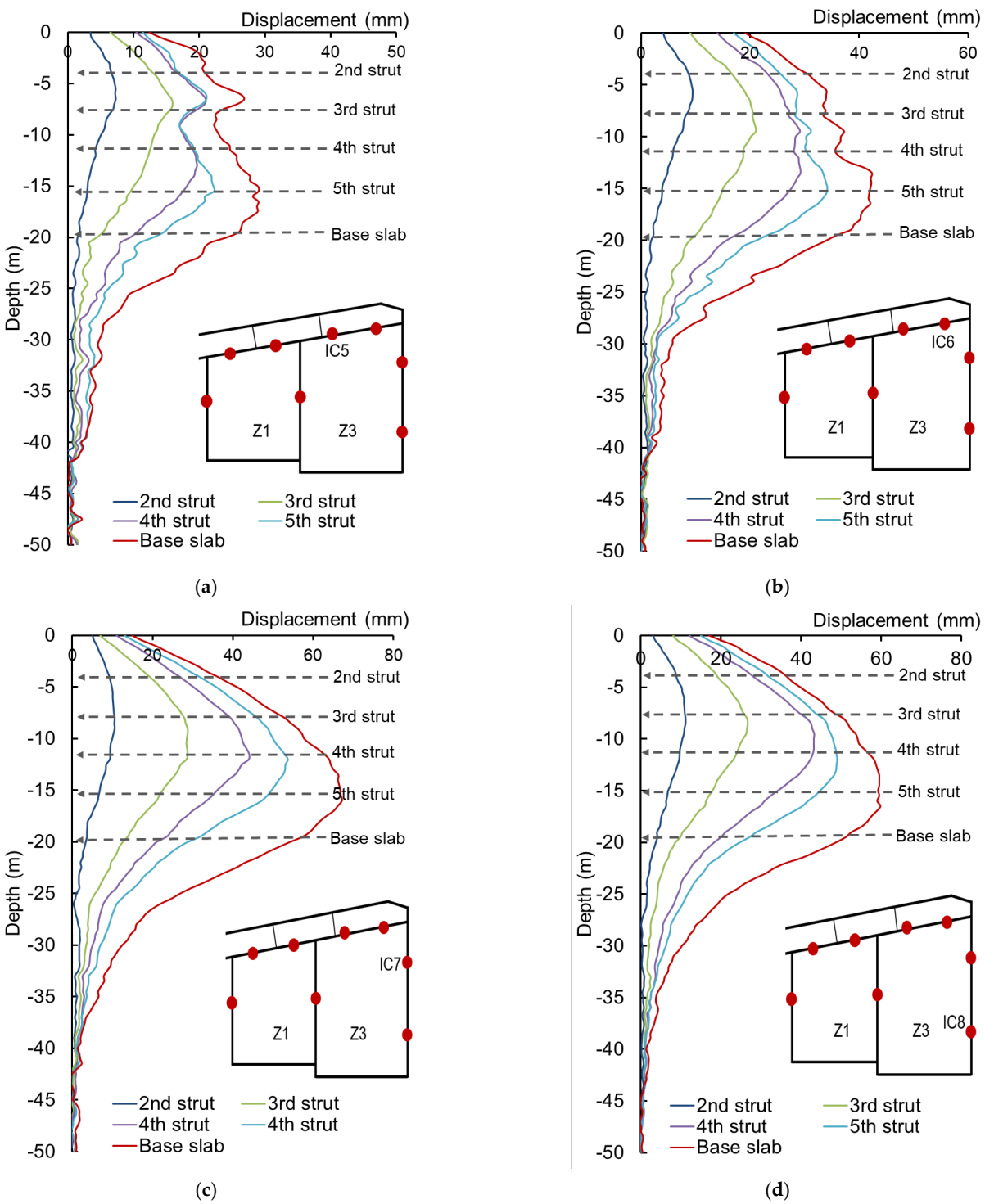

Figure 8. Wall horizontal displacement results of the foundation pit Z3: (**a**) Point IC5; (**b**) Point IC6; (**c**) Point IC7; (**d**) Point IC8.

4.1.2. Assessing the Performance of the Servo Strut System

A comparison of the wall displacement results in the two pit zones Z1 and Z3 helps to evaluate the functionality of the servo bracing system. The most obvious distinction is that servo forces alter the flexural behavior of the diaphragm wall, which causes several local inflection points (at the positions of servo jacks), such as in the result plots corresponding to the time stages of the fourth and fifth strut and the base slab in Figure 8a,b. In contrast, the flexural curves plotted in Figure 7a,b are smoother and have no inflection

points. Furthermore, the servo forces can reduce the overall deformation extent of the wall, and hence help mitigate the impacts of pit excavation on the surrounding ground. For instance, if comparing the displacement results at IC1 and IC6, the peak displacements by the excavation to 19.9 m BGS reach approximately 54 mm and 42 mm, respectively, while at IC2 and IC5 (where servo forces are imposed) they reach about 42 mm and 29 mm, respectively. This indicates the servo struts reduce the maximum wall displacement by about 22% at IC1 and IC6, and by 31% at IC2 and IC3.

In addition, the impacts of the servo forces also vary with different servo jack configurations. Observing the wall deformation results in Figure 8, it can be revealed that, on the north side of pit Z3, where servo forces are imposed at the third/fourth/fifth struts, the displacement plots at IC5 and IC6 have more local inflection points, while at IC7 and IC8, where only the fourth strut is imposed servo forces, the displacement curves (see Figure 8c,d) are highly smooth as those in Figure 7, with no significant inflection points. Notably, it is not reasonable to assess the performance of servo jacks by comparing the displacement at IC3, IC4, IC7, and IC8, because a large distinction already exists in the initial displacement evolution of these measurement points, which occurred before the servo forces were activated at pit Z3. However, if only observing the displacement evolution after activating the fourth strut, it can be seen that, without the servo system, the increment of peak displacements at IC3 and IC4 in pit Z1, from the fourth strut to the depth of 19.9 m, are 59 mm and 27 mm; in contrast, with the servo force system, the increments in peak displacements at IC7 and IC8 in pit Z3 are of 22 mm and 16 mm, and this implies that the servo jacks play a role in mitigating the displacement evolution afterward.

Furthermore, the servo forces also alter the deflection mode of the wall, by driving the location of the peak displacement upward. For instance, from the plots in Figure 7, without servo forces, the depths of peak displacement at IC1 to IC4 are of 21.5 m, 19.0 m, 21.0 m, and 20 m BGS, generally below (or very close to) the excavation depth of 19.9 m BGS. However, as can be seen from Figure 8, with imposed servo forces, the depths of peak displacement at IC5 to IC8 are 13 m, 15.0 m, 15.5 m, and 13.5 m BGS, generally far above the excavation depth of 19.9 m BGS.

4.1.3. Displacement Evolution of Characteristic Depths with Servo Strut

In addition to the overall wall displacement curves measured by inclinometers (displayed in Figures 8 and 9), the effects of the servo forces on the wall displacement are further analyzed by observing the displacement evolution at selected (characteristic) depths in the diaphragm wall, which corresponds to the positions of the servo jacks (depths of the third to fifth concrete struts). In this project, the data from the inclinometers casting IC5 to IC8 in foundation pit Z3 are specified in Figure 9, and it can be noted that the starting day (Day 0) corresponds to the start of the pit Z3 excavation.

The displacement evolution tendency after imposing servo forces is the focus of this analysis. When the individual hydraulic jack at the third strut is loaded from an initial 1 MN (Meganewton) on Day 29 to a final 3 MN by Day 34, the wall displacement of IC5 (in Figure 9a) only changes from 17.3 mm to 18.7 mm in these 5 days, with an increment of 1.4 mm, whereas the wall displacement increment within the 5 days (before Day 29) is of about 2.2 mm. Furthermore, observing the displacement curves of the fourth and the fifth struts at IC5, the displacement increments are of 2.4 mm and 1.8 mm, respectively, after imposing the servo forces at the third strut, corresponding to the displacement increments of 4.0 mm and 2.8 mm at the same time-interval before. At IC6 in Figure 9b, the wall displacement shows a similar characteristic, as the servo forces tend to flatten the displacement curve and mitigate its gradient afterward.

In addition, when the jacks at the fourth strut are loaded to 1 MN on Day 46 to 2.5 MN by Day 48, the displacement curve of IC5 exhibits a significant decrease, say 2.6 mm at the depth of the third strut, 2.9 mm at the fourth strut, and only 0.7 mm at the fifth strut, which indicates that the loading of the fourth strut imposes less effects on the fifth strut. At IC6 in Figure 9b, the wall displacement shows a rather similar characteristic under the

servo forces, and a distinguishable decrease occurs in the curves of the third and the fourth struts, but its influence on the fifth strut is insignificant. Overall, the wall displacement curves are flattened significantly by the imposed servo forces, which demonstrates that the servo concrete strut effectively assists in controlling wall displacements, and thus mitigates the disturbance to the surrounding grounds.

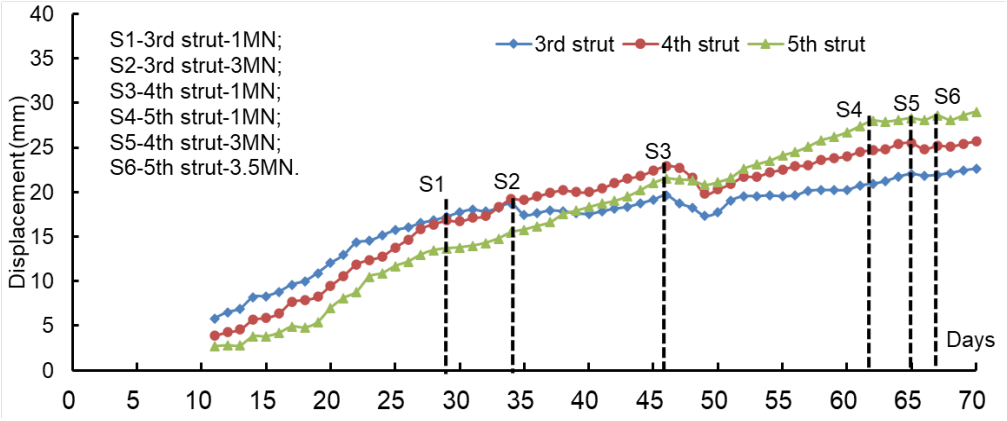

(**a**)

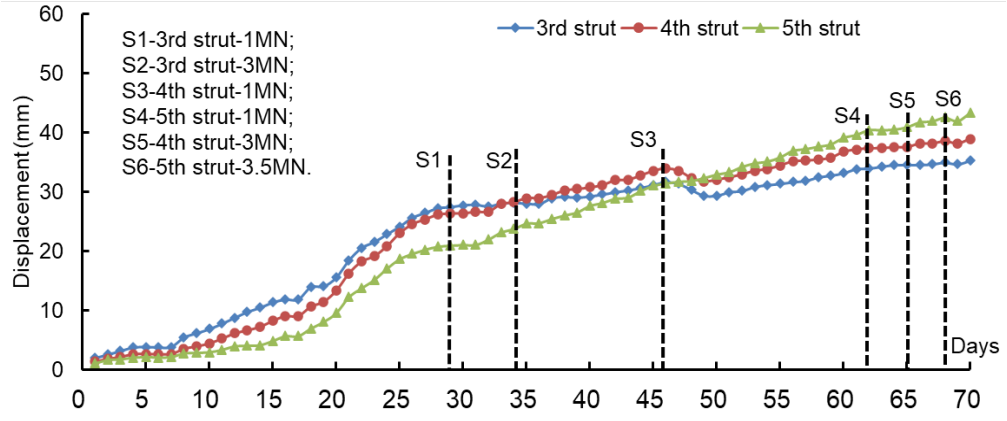

(**b**)

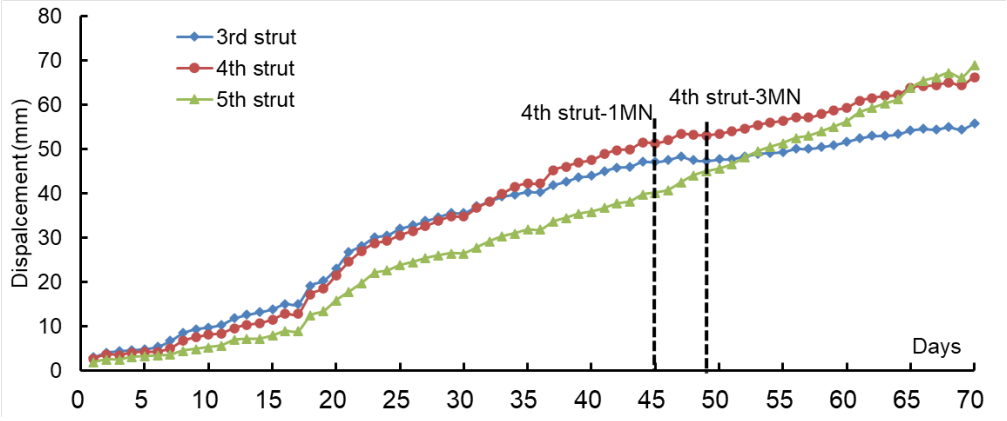

(**c**)

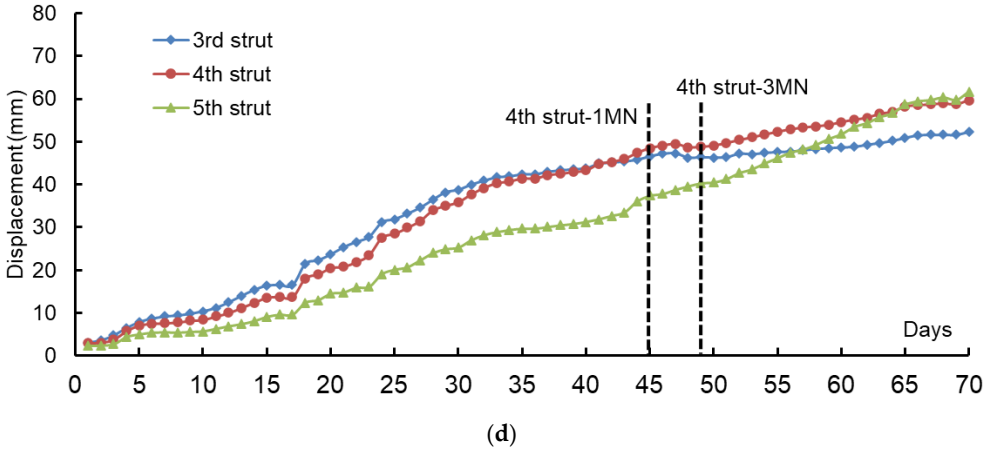

(**d**)

Figure 9. Displacement evolution at strut depths of the wall in foundation pit Z3: (**a**) Measurement point IC5; (**b**) Measurement point IC6; (**c**) Measurement point IC7; (**d**) Measurement point IC8.

Figure 9c,d demonstrates the wall displacement measured at IC7 and IC8. The servo forces are only acting on the fourth strut, and it can be shown that the forces impose more significant effects on the third and fourth struts than on the fifth strut. The servo forces flatten the displacement curves corresponding to the third and fourth struts, and at IC7 the average daily increment of displacement was reduced from about 0.6 mm (period of Day 41–45) to 0.45 mm (period of Day 45–49) at the fourth strut, and from about 0.5 mm to 0 mm at the third strut. However, its impacts on the fifth strut seem insignificant, and comparing the displacement curves monitored on the north and east sides, it can be inferred that the servo jacks, when configured to multiple layers vertically, have a higher effectiveness in mitigating wall displacement than when to a single layer.

4.2. Discussion

The servo concrete strut developed in this study has demonstrated effectiveness in mitigating diaphragm wall displacements, and hence a highly promising technique applicable in braced pit excavation projects. Compared with other technical measures to mitigate wall displacement, such as conducting soil reinforcement (using deep soil mixing or jet grouting et al.), constructing a stiffer bracing structure (with thicker walls or additional layers of struts), implementing servo jacks is a competent alternative since it assures a relatively more reliable performance control than deep soil reinforcement, and eliminates the needs of constructing additional layers of struts (and hence a wider workspace). Specifically, the imposed servo forces can be adjusted alongside with construction stages, which can help maintain sufficient support to the wall, especially given the negative effects of concrete thermal shrinkage (in cold periods); moreover, if the servo forces are imposed properly, the stiffness of the whole bracing system can be boosted, and it can offer a higher resistance to the ongoing ground deformation.

However, there exist several issues relating to design optimization and safety control of servo struts which deserve further discussion. First and foremost, the level of servo force exhibits influences on the whole bracing system stability. For example, a too-high servo force may punch the concrete wall and cause local cracking, deteriorate its watertightness, and even result in a fatal collapse; furthermore, a high servo force introduces excessive compressive forces on the struts, which may cause cross-section damage. In summary, a proper force-loading scheme plays a vital role when implementing the servo-type bracing system.

To address these limitations or risks, some specific optimization works are recommended. Firstly, when assembling the hydraulic jacks with the concrete wall and struts, measures should be taken to mitigate the stress concentration on the jack–wall contact face, such as by adding a steel buffering pad to disperse the jacking force more uniformly.

Secondly, in servo concrete struts, as presented in Figure 6b, purlins will detach from the wall and this detachment may result in risks of collapsing. For instance, in this case study a maximum of 70 mm gap was observed in the field. Therefore, adding more physical constraints to the purlins is preferred, such as by constructing more temporary columns on the vertical plane and struts on the horizontal plane. For further application, a theoretical or numerical simulation model is recommended, which assists in initially assessing the effects of servo forces on wall deformation when scheming the loading procedures. Considering the complexity of geotechnical design, it will be beneficial to engineers if an artificial intelligence (AI)-based training program can be investigated [21,22], which preferably links the system performance with critical design parameters such as soil physical properties, excavation depth, and bracing structure parameters.

Finally, when implementing servo concrete struts in braced excavation projects, timely monitoring work is critical for ensuring the safety and stability of the whole bracing system. The monitoring work has to cover important parameters ranging from wall lateral displacements, the detachment clearance of the wall–purlin contact face, axial forces of structs, and nearby ground deformations. Notably, this monitoring work not only helps learn about the bracing structure behaviors, but also contributes to optimizing the soil excavation scheming for ground disturbance mitigation. Last but not least, this study is primarily confined to evaluating the performance of servo struts through field measurements, and it does not address other important issues relevant to its future engineering applications, such as developing a numerical model and proposing technical manuals or guidelines, which will become the meaningful parts of future research.

5. Conclusions

This study demonstrates the world's first development case of a servo concrete bracing system for foundation pit excavation in geotechnical engineering. The system configuration and design philosophy are described, and its technical performance is investigated through field monitoring studies, where the servo concrete strut system is implemented successfully in an actual deep foundation pit project in Shanghai, China. The project background information is first introduced, followed by detailing the servo concrete bracing system. Subsequently, extensive field monitoring results are presented and analyzed to specifically evaluate the technical performance of this servo bracing system, which serves as a valuable reference to the geotechnical engineering community.

The following conclusions can be drawn from this study:

(1) The servo concrete bracing system, which is successfully applied in this study, is composed of reinforcement concrete struts, revised purlins, hydraulic jacks, and hydraulic pumping parts. The field implementation demonstrates that this novel servo bracing system is effective in mitigating the wall displacement in foundation pit excavation.

(2) The servo hydraulic forces alter the retaining wall's flexural behavior, by triggering several local inflection points at the depths of servo jacks. Furthermore, the servo forces can reduce the overall scale of the wall deformation and help mitigate the disturbance of excavation. Under a quantitative evaluation, the servo forces can reduce the maximum wall displacement by as much as 31% in the case study. Additionally, the servo forces also alter the wall's deflection mode by driving the location of the peak displacement upward.

(3) The performance of the servo struts shows variations in different jack configurations. Specifically, the servo jacks configured to multiple layers of struts have a higher effectiveness in mitigating wall displacement than to a single layer. Moreover, the servo forces not only impact the corresponding strut but also affect the adjacent struts' behavior. This implies that the monitoring scope should be expanded when applying the servo strut system in actual foundation pit engineering.

Author Contributions: Conceptualization, S.W. and X.Z. (Xuehui Zhang); methodology, S.W., L.X., and X.Z. (Xuehui Zhang); validation, S.W., X.Z. (Xuehui Zhang), and L.L.; formal analysis, S.W., X.Z., (Xuehui Zhang) and L.L.; resources, S.W. and L.X.; data curation, S.W. and L.X.; writing—original draft preparation, S.W., X.Z. (Xuehui Zhang), and L.L.; writing—review and editing, X.Z. (Xuehui Zhang) and X.Z. (Xiaoying Zhuang); visualization, X.Z. (Xuehui Zhang) and L.L.; supervision, S.W. and X.Z. (Xiaoying Zhuang). All authors have read and agreed to the published version of the manuscript.

Funding: This research received no external funding.

Data Availability Statement: The data are not publicly available due to privacy.

Conflicts of Interest: Author Shaochun Wang was employed by the company Shanghai Construction No. 1 (Group) Co., Ltd. The remaining authors declare that the research was conducted in the absence of any commercial or financial relationships that could be construed as a potential conflict of interest.

References

1. Zhang, Z.; Huang, M.; Wang, W. Evaluation of deformation response for adjacent tunnels due to soil unloading in excavation engineering. *Tunn. Undergr. Space Technol.* **2013**, *38*, *244–253*. https://doi.org/10.1016/j.tust.2013.07.002.
2. He, H.; Wang, S.; Shen, W.; Zhang, W. The influence of pipe-jacking tunneling on deformation of existing tunnels in soft soils and the effectiveness of protection measures. *Trans. Geotech.* **2023**, *42*, 101061.
3. Mi, C.; Liu, Y.; Zhang, Y.; Wang, J.; Feng, Y.; Zhang, Z. A vision-based displacement measurement system for foundation pit. *IEEE Trans. Instrum. Meas.* **2023**, *72*, 1–15.
4. Xu, D.; Zhang, X.; Chen, W.; Jiang, X.; Liu, Z.; Bai, Y. Utilisation of the deep underground space in Shanghai. *Proc. Inst. Civ. Eng. Munic. Eng.* **2019**, *172*, 218–223.
5. Zhang, X.; Zhu, H.; Jiang, X.; Broere, W. Distributed fiber optic sensors for tunnel monitoring: A state-of-the-art review. *J. Rock Mech. Geotech. Eng.* **2024**. https://doi.org/10.1016/j.jrmge.2024.01.008.
6. Zhu, H.H.; Wang, D.Y.; Shi, B.; Wang, X.; Wei, G.Q. Performance monitoring of a curved shield tunnel during adjacent excavations using fiber optic nervous sensing system. *Tunn. Undergr. Space Technol.* **2022**, *124*, 104483.
7. Jiang, X.; Zhang, X.; Zhang, X.; Long, L.; Bai, Y.; Huang, B. Advancing Shallow Tunnel Construction in Soft Ground: The Pipe-Umbrella Box Jacking Method. *Transp. Res. Rec.* **2024**. https://doi.org/10.1177/03611981231225430.
8. Song, D.; Chen, Z.; Dong, L.; Tang, G.; Zhang, K.; Wang, H. Monitoring analysis of the influence of extra-large complex deep foundation pit on adjacent environment: A case study of Zhengzhou City, China. *Geomat. Nat. Haz. Risk.* **2020**, *11*, 2036–2057. https://doi.org/10.1080/19475705.2020.1823492.
9. Zhang, X.; Yang, J.; Zhang, Y.; Gao, Y. Cause investigation of damages in existing building adjacent to foundation pit in construction. *Eng. Fail. Anal.* **2018**, *83*, 117–124. https://doi.org/10.1016/j.engfailanal.2017.09.016.
10. Meng, F.Y.; Chen, R.P.; Xu, Y.; Wu, K.; Wu, H.N.; Liu, Y. Contributions to responses of existing tunnel subjected to nearby excavation: A review. *Tunn. Undergr. Space Technol.* **2022**, *119*, 104195. https://doi.org/10.1016/j.tust.2021.104195.
11. Moormann, C. Analysis of wall and ground movements due to deep excavations in soft soil based on a new worldwide database. *Soils Found.* **2004**, *44*, 87–98. https://doi.org/10.3208/sandf.44.87.
12. Liu, G.; Wang, W. *Foundation Pit Engineering Handbook*, 2nd ed.; China Architecture & Building Press: Beijing, China, 2009. (In Chinese)
13. Jin, Y.; Zhang, Y.; Yan, J.; Wang, H.; Cheng, W. Application of New Steel Support Axial Force Servo System in Deep Foundation Pit Adjacent to Subway. *Build. Constr.* **2021**, *43*, 2040–2042. https://www.hindawi.com/journals/ace/2022/1243282/. (In Chinese)
14. Zhai, J.; Jia, J.; Xie, X. Practical research of concrete strut with automatic axial force compensation system in a deep excavation project. *Build. Struct.* **2022**, *52*, 148–152. https://link.oversea.cnki.net/doi/10.19701/j.jzjg.YG220115. (In Chinese)
15. Li, M.G.; Demeijer, O.; Chen, J.J. Effectiveness of servo struts in controlling excavation-induced wall deflection and ground settlement. *Acta Geotech.* **2020**, *15*, 2575–2590. https://doi.org/10.1007/s11440-020-00941-9.
16. Zhang, G.; Su, D.; Pang, X.; Yang, Q.; Zhou, Q. The Influence of Axial Force Servo System in Excavation of Foundation Pit on the Deformation of Existing Subway Tunnel. *Mod. Tunn. Technol.* **2020**, *57*, 521–527. (In Chinese) https://link.oversea.cnki.net/doi/10.13807/j.cnki.mtt.2020.S1.069.
17. Nangulama, H.K.; Jian, Z. Deformation control monitoring of basement excavation at field construction site: A case of hydraulic servo steel enhancement geotechnology. *Adv. Civ. Eng.* **2022**, *2022*, 6234581. https://doi.org/10.1155/2022/6234581.
18. Di, H.; Jin, Y.; Zhou, S.; Zhang, X.; Wu, D.; Guo, H. Experimental study on the adjustments of servo steel struts in deep excavations. *Acta Geotech.* **2023**, *18*, 6615–6629. https://doi.org/10.1007/s11440-023-01959-5.
19. *GB 50021-2001*; Chinese Code for Investigation of Geotechnical Engineering, 2009 ed. Ministry of Housing and Urban-Rural Development: Beijing, China, 2009. (In Chinese)
20. *GB/T 50123-2019*; Chinese Standard for Geotechnical Testing Method. Ministry of Housing and Urban-Rural Development: Beijing, China, 2019. (In Chinese)

21. Nguyen Van, C.; Keawsawasvong, S.; Nguyen, D.K.; Lai, V.Q. Machine learning regression approach for analysis of bearing capacity of conical foundations in heterogenous and anisotropic clays. *Neural Comput. Appl.* **2023**, *35*, 3955–3976.
22. Su, Y.; Wang, J.; Li, D.; Wang, X.; Hu, L.; Yao, Y.; Kang, Y. End-to-end deep learning model for underground utilities localization using GPR. *Autom. Constr.* **2023**, *149*, 104776.